*J. Plasma Physics* (2000), *vol.* 64, *part* 4, *pp.* 459–474. Printed in the United Kingdom 
© 2000 Cambridge University Press

# Turbulent adiabatic shock waves and diffusive particle acceleration

I. LERCHE,* M. POHL and R. SCHLICKEISER

Institut für Theoretische Physik, Lehrstuhl IV: Weltraum- und Astrophysik,
Ruhr-Universität Bochum, D-44780 Bochum, Germany

(Received 31 May 2000 and in revised form 14 August 2000)

**Abstract.** We investigate the properties of turbulent adiabatic shock waves resulting from the self-consistent inclusion of finite Alfvén-wave pressure in the shock balance equations. We demonstrate (i) the absence of a switch-on shock; (ii) the existence of two separated domains where the Mach number is greater than unity that have gas compression, and an associated domain where the gas compression ratio is less than unity (i.e. a rarefaction domain); (iii) the difference between the scattering-centre compression ratio and the gas compression ratio for all upstream wave cross-helicity values except for the isolated case of zero helicity; (iv) the presence of anomalous domains where the cosmic-ray particle spectral index can be negative. All of these results are brought about by including the upstream and downstream turbulent wave energies in the shock balance structure. Without the waves, none of the effects persists.

## Dedication

This paper is dedicated to John Dougherty on the occasion of his 65th birthday. One of the authors (I.L.) is particularly grateful to John, who was his external PhD examiner many years ago (1965). Despite errors in the thesis, John allowed acceptance of the work. Hopefully this work has fewer errors – so that one has learnt from the experience. Thank you, John.

## 1. Introduction

Acceleration at collisionless astrophysical shock waves is regarded as a universal mechanism to generate high-energy charged particles in cosmic plasmas (for reviews, see Drury 1983; Blandford and Eichler 1987; Jones and Ellison 1991). Progress in understanding the properties of the resulting energy spectra of the accelerated particles is closely related to the properties of the astrophysical shock waves. On the one hand, there is compelling observational evidence from radio emission studies of many tens of supernova remnants in our Galaxy and in other galaxies that the spectral indices of at least relativistic electrons are largely independent

* Permanent address: Department of Geological Sciences, University of South Carolina, Columbia, SC 29208, USA.

https://doi.org/10.1017/S0022377800008801 Published online by Cambridge University Press

of age, size, luminosity, or other evolutionary parameters. Accordingly, sustained particle acceleration at shock fronts is required to account for the preponderance of the observations. Investigations in this direction have been made by Dröge et al. (1987) and Schlickeiser and Fürst (1989). On the other hand, it is also clear from observations (Kennel et al. 1986) and from basic theoretical considerations (McKenzie and Westphal 1969; Scholer and Belcher 1971; Achterberg and Blandford 1986; Vainio and Schlickeiser 1998) that there exists significant turbulent wave energy both ahead of an evolving shock (i.e. in the unperturbed interplanetary or interstellar medium ahead of the shock) and behind the shock. The self-consistent treatment of charged-particle acceleration in such settings is critical, as pointed out by Vainio and Schlickeiser (1999 – hereafter referred to as VS), because the changes in turbulence wave spectra across the shock influence not only the particle energy spectra but also the self-consistent shock dynamics, which produces significant modifications to particle acceleration results that arise from a test-particle approach.

In an investigation of the self-consistent wave effects on the shock, and so on the charged-particle spectra, VS followed an approach pioneered by Scholer and Belcher (1971). Two major results were derived from the self-consistent inclusion of wave effects.

1. VS derived an equation (their equation (13)) relating the Alfvénic shock Mach number $M$ to the plasma $\beta$ factor ($P = \beta\rho V_A^2/\gamma$), the gas adiabatic index $\gamma$, ($P\rho^{-\gamma} =$ constant), the gas compression ratio $r$, and the normalized upstream wave magnetic field $b = (\delta B_1/B_0)^2$ in the form

$$\begin{aligned}&(M^2 - r)^2\{2r\beta - M^2[\gamma + 1 - (\gamma - 1)r]\}\\ &+bM^2r\{(\gamma - 1)r^2 + [M^2(2 - \gamma) - (\gamma + 1)]r + \gamma M^2\} = 0.\end{aligned} \tag{1}$$

   Apart from the definition of the upstream turbulence parameter $b$, the notation here is that used by VS. Substituting

$$M^2 = ru, \tag{2}$$

   simple rearrangement allows the cubic equation (1) to be written in the form

$$M^2 = \frac{(u - 1)^2[u(\gamma + 1) - 2\beta] + bu[\gamma + 1 - \gamma u]}{(\gamma - 1)(u - 1)^2 + b[\gamma - 1 + u(2 - \gamma)]} \equiv \frac{N}{D}. \tag{3}$$

2. After specifying the upstream Alfvén wave cross-helicity state $H_{c,1}$, which indicates the relative fraction of forward- and backward-moving Alfvén waves so that the upstream cosmic-ray bulk speed is $V_1 = U_1 + H_{c,1}V_{A,1}$ in terms of the upstream gas speed $U_1$ and Alfvén velocity $V_{A,1}$, VS calculated the resulting downstream cosmic-ray bulk speed $V_2 = U_2 + H_{c,2}V_{A,2}$ from the shock jump conditions. This immediately yielded the scattering-centre compression ratio

$$R \equiv \frac{V_1}{V_2} = r\,\frac{M + H_{c,1}}{M + r^{1/2}H_{c,2}}, \tag{4}$$

   which in general is different from the gas compression ratio $r$. Because the shock wave is collisionless, it is this scattering-centre compression ratio, and not the gas compression ratio, that determines the spectral index of the power-

https://doi.org/10.1017/S0022377800008801 Published online by Cambridge University Press

law momentum spectrum of the accelerated cosmic-ray particles, $\Gamma$, simply through (Drury 1983; Schlickeiser et al. 1993)

$$\Gamma = \frac{R+2}{R-1}. \tag{5}$$

The primary purpose of this paper is to investigate in more detail than given in VS the structural details of the shock cubic (3), because the particle spectral index and also the types of self-consistent shock behaviour available are remarkably sensitive to the precise values and ranges of the gas adiabatic index $\gamma$ and the upstream turbulence parameter $b$.

## 2. The absence of a 'switch-on' shock

Boyd and Sanderson (1969) noted that in the *absence* of any upstream wave magnetic field (i.e. $b = 0$), (3) reduces to

$$M^2 = \frac{u(\gamma+1) - 2\beta}{(\gamma-1)},$$

which, as $u \to 1$, reduces to

$$M^2 = \frac{(\gamma+1) - 2\beta}{\gamma - 1}, \quad \text{and then} \quad r = M^2. \tag{6}$$

Because of the requirement that $M^2 \geqslant 1$, one then requires $\gamma - 1 \leqslant \gamma + 1 - 2\beta$ or consequently $\beta \leqslant 1$ for such a switch-on shock to exist.

However, note that for any finite value of the turbulence parameter $b$, no matter how small, as $u \to 1$, the general equation (3) reduces to

$$M^2 = \frac{b}{b} = 1, \quad \text{and} \quad r = 1. \tag{7}$$

Thus, *physical existence is not possible for a switch-on shock in the presence of any level of upstream wave magnetic field.* This simple result is a consequence of including the self-consistent Alfvén waves in the analysis of the shock conditions, and is a result that cannot be produced without including the wave energy. As such, this result provides a sharp lesson in the need to use such a self-consistent approach.

## 3. Shock properties for $1 \leqslant \gamma \leqslant 2$

The special end values $\gamma = 1$ and $\gamma = 2$ are best treated separately, although, as will be shown a little later, they can be incorporated within the same topological picture as results for $1 < \gamma < 2$.

### *3.1. The case $\gamma = 1$*

In this situation, (3) reduces to

$$M^2 = \frac{2(u-1)^2(u-\beta) + bu(2-u)}{bu}. \tag{8}$$

The requirement that $M^2 \geqslant 1$ then places a constraint on (8), namely that

$$2(u-1)^2(u-\beta) \geqslant bu(u-1). \tag{9}$$

https://doi.org/10.1017/S0022377800008801 Published online by Cambridge University Press

Note from (8) that, at $u = 1$, $M^2 = 1$, and that $(dM^2/du)|_{u=1} = -1$, so that near $u = 1$, $M^2 \simeq 2 - u$ is *decreasing* from 1+ to 1− as $u$ increases from 1− to 1+. Note also from (8) that as $u \to 0$, $M^2 \to 2 - 2\beta/bu$, so that $M^2$ will cross unity below $u = 1$, at about $u \simeq 2\beta/b$ for $\beta \leqslant \frac{1}{2}b$. Note also that as $u \to \infty$, $M^2 \to 2u^2/b \gg 1$, so that $M^2$ must have at least one minimum in the range $u > 1$.

For large values of $\beta \gg 1$, the first term in the numerator of (8) is large and negative for all $u < \beta$, and dominates the numerator except for a strip centred around $u = 1$ of halfwidth $\Delta u \simeq [b/2(b + \beta)]^{1/2} \simeq (b/2\beta)^{1/2} \ll 1$ where the second term dominates. Hence, between $u = 1 - \Delta u$ and 1, $M^2$ crosses unity.

For $\beta = 2$, (8) takes the form

$$M^2 = \frac{(u-2)[2(u-1)^2 - bu]}{bu}, \tag{10}$$

which has zeros at $u = 2$ and at

$$u_\pm = 1 + \tfrac{1}{4}b \pm \tfrac{1}{4}(8b + b^2)^{1/2},$$

with $u_+ > 1$ and $u_- < 1$. A sketch of the behaviour of $M^2$ with $u$ for various values of $\beta$ and $b$ is given in Fig. 1.

### *3.2. The case $\gamma = 2$*

In this special situation, (3) reduces to

$$M^2 = \frac{(u-1)^2(3u - 2\beta) + bu(3 - 2u)}{(u-1)^2 + b} = \frac{N}{D}. \tag{11}$$

Note that as $u \to 0$, $N \to -2\beta$, while $D \to 1 + b$, so $M^2 \to -2\beta/(1 + b)$; at $u = 1$, $M^2 = 1$, so that between $u = 0$ and $u = 1$, $M^2$ must cross zero. Note that $(dM^2/du)|_{u=1} = -1 < 0$, so that $M^2$ is decreasing through unity as $u$ increases through unity.

For $\beta = \frac{9}{4}$, (11) reduces to

$$M^2 = \frac{(3 - 2u)[bu - \frac{3}{2}(u-1)^2]}{(u-1)^2 + b}, \tag{12}$$

which has zeros at $u = \frac{3}{2}$ and at

$$u_\pm = 1 + \tfrac{1}{3}b \pm \tfrac{1}{3}(6b + b^2)^{1/2}. \tag{13}$$

Note that $u_+ > 1$ (and $u_+ > \frac{3}{2}$ when $b > \frac{1}{4}$), and $0 < u_- < 1$ always.

For $\beta \neq \frac{9}{4}$, two extreme limits exist. For $\beta \ll 1$, the first term of $N$ in (11) is positive for $u > \frac{2}{3}\beta$, while the second term turns negative only when $u > \frac{3}{2}$. Hence, $M^2$ crosses zero close to $u = 0$ at about

$$u_0 \simeq \frac{2\beta}{3(1 + b) + 4\beta} \ll 1. \tag{14}$$

For $\beta \gg 1$, the first term in $N$ is negative until $u > \frac{2}{3}\beta \gg 1$, and dominates the second term (for $\beta \gg b$) except in a narrow region around $u = 1$, of width $\Delta u \simeq [2b/(\beta + b)]^{1/2}$. A sketch of the behaviour of $M^2$ versus $u$ is shown in Fig. 2 for various values of $\beta$ and $b$.

https://doi.org/10.1017/S0022377800008801 Published online by Cambridge University Press

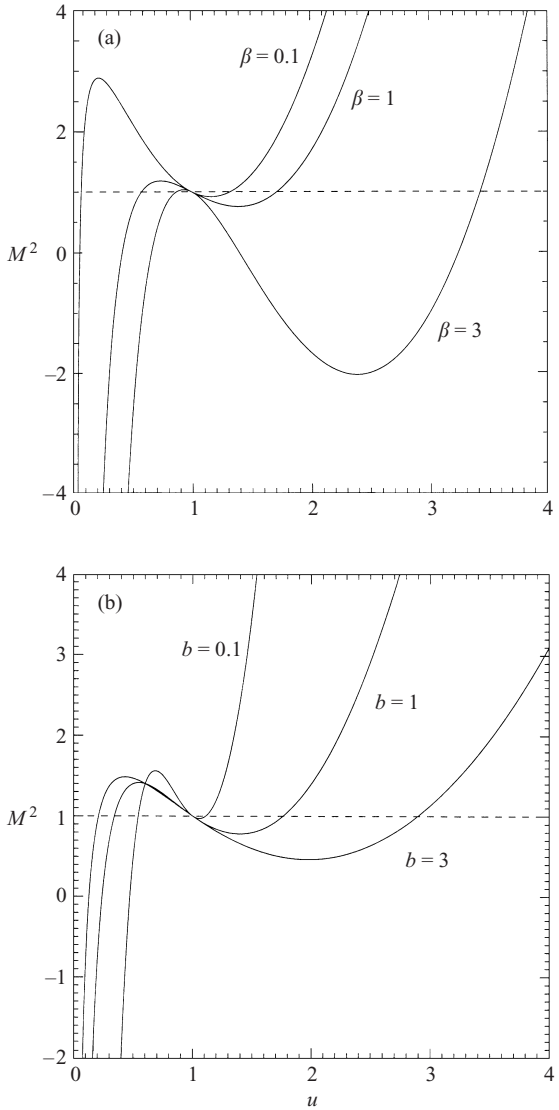



**Figure 1.** Plots of $M^2$ versus $u$ for the case $\gamma = 1$: (a) for $b = 0.6$ for various values of the plasma beta $\beta$; (b) for $\beta = 0.6$ for various values of the turbulence parameter $b$. Only the regions with $M^2 \geqslant 1$ (represented by the dashed line at $M^2 = 1$) represent physically acceptable domains.

### *3.3. The case* $1 < \gamma < 2$

In this case, the full aspects of (3) must be used. Note, however, that in $1 < \gamma < 2$, the factor $D$ in (3) is intrinsically positive. A special situation occurs when $\beta = (\gamma + 1)^2/2\gamma$, because (3) can then be written

$$M^2 = \frac{(\gamma + 1 - \gamma u)\left[\dfrac{\gamma + 1}{\gamma}(u - 1)^2 - bu\right]}{(\gamma - 1)(u - 1)^2 + b[\gamma - 1 + u(2 - \gamma)]}, \tag{15}$$

https://doi.org/10.1017/S0022377800008801 Published online by Cambridge University Press

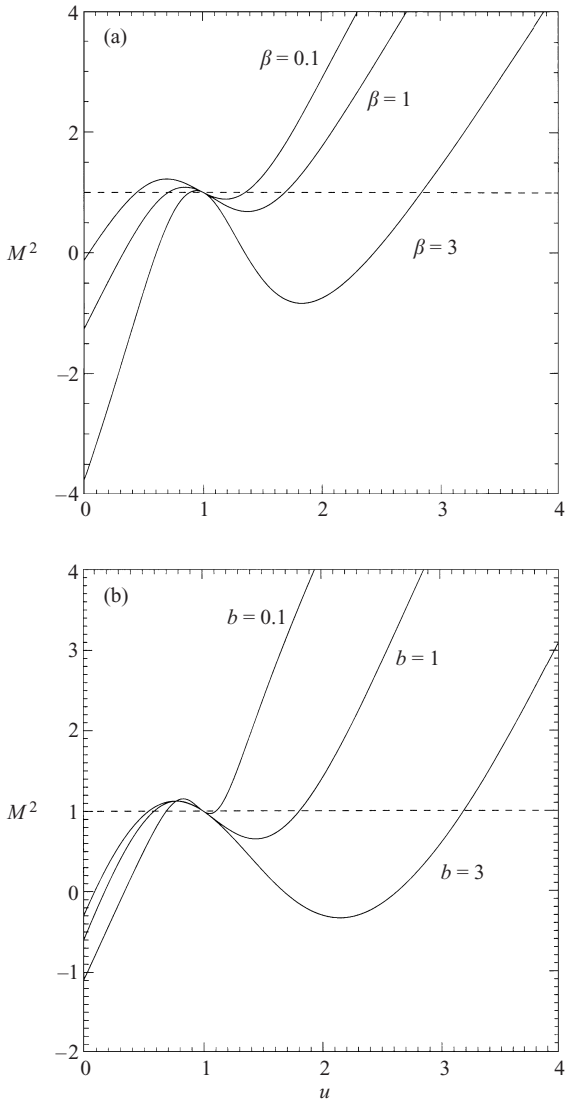



**Figure 2.** Plots of $M^2$ versus $u$ for the case of $\gamma = 2$: (a) for $b = 0.6$ for various values of the plasma beta $\beta$; (b) for $\beta = 0.6$ for various values of the turbulence parameter $b$. Only the regions with $M^2 \geqslant 1$ (represented by the dashed line at $M^2 = 1$) represent physically acceptable domains.

with zeros at $u_1 = (\gamma + 1)/\gamma > 0$ and at

$$u_\pm = 1 + \frac{\gamma b}{2(\gamma + 1)} \pm \frac{1}{2(\gamma + 1)}[4(\gamma + 1)\gamma b + (\gamma b)^2]^{1/2}, \tag{16}$$

which includes as special cases (10) and (13) for $\gamma = 1$ and $\gamma = 2$, respectively. The relative positioning of $u_1$ with respect to $u_+$ depends on the value of $b$. If $b > (\gamma + 1)/[\gamma^2(\gamma - 1)]$ then $u_+ > u_1 > 1$, while if $b < (\gamma + 1)/[\gamma^2(\gamma - 1)]$ then $u_1 > u_+ > 1$.

https://doi.org/10.1017/S0022377800008801 Published online by Cambridge University Press

For the more general situation of $\beta \neq (\gamma+1)^2/2\gamma$, again, just as in the $\gamma = 2$ case, two extreme situations depict the behaviour of $M^2$. For $\beta \ll 1$, the first factor in $N$ of (3) is positive for $u > 2\beta/(\gamma+1)$ while the second factor in $N$ does not turn negative until $u > 1 + \gamma^{-1}$. At $u = 0$, $M^2 = -2\beta/[(\gamma-1)(1+b)] < 0$, so that $M^2$ crosses zero before $u = 2\beta/(\gamma+1)$ is reached. For $\beta \gg 1$, the first term is negative and dominates $N$ except in a small region around $u = 1$, of width $\Delta u \simeq 2[b/(2\beta + b\gamma)]^{1/2}$ where the second term controls $N$.

In all cases with $1 < \gamma < 2$, there is a domain of $u < 1$ where $M^2 > 1$. For this domain, $M^2$ crosses unity at

$$u_2 = \frac{1}{2(\gamma+1)}\left(b\gamma + 2(\beta+\gamma) - \{[b\gamma + 2(\beta-1)]^2 - 4b(\gamma+1)\}^{1/2}\right) \tag{17}$$

Hence, in $u_2 \leqslant u \leqslant 1$, $M^2 > 1$ represents one of the physically allowed domains. Figure 3 shows the behaviour for $\gamma = 1.5$ of $M^2$ versus $u$ for various values of $\beta$ and $b$.

## 4. Shock properties for $\gamma > 2$

The situation of an adiabatic index $\gamma > 2$ is not so often encountered, because independent non-relativistic particles have $\gamma = \frac{5}{3}$. However, under collective motion of particles, it is possible to have an equivalent adiabatic index that is extremely large – such as, for example, for a constant-density solid, represented by $\gamma \to \infty$. Thus, in the interests of completeness, it is appropriate to give a short discussion on the anomalous case $\gamma > 2$.

Because the denominator in (3) is of the form

$$D = (\gamma-1)(u-1)^2 + b[\gamma - 1 - u(\gamma-2)], \tag{18}$$

once that $\gamma > 2$, it is possible for $D$ to possess zeros in addition to the numerator $N$. Any zeros of $D$ occur when

$$b = \frac{(\gamma-1)(u-1)^2}{(\gamma-2)\left(u - \dfrac{\gamma-1}{\gamma-2}\right)}, \tag{19}$$

which requires $u > u_0 = (\gamma-1)/(\gamma-2)$ as a necessary condition. Note that when $u > u_0$, (19) has a minimum as $u$ varies in $\infty > u > u_0$ occurring at $u_{\min} = 2u_0 - 1 = \gamma/(\gamma-2) > 1$, with

$$b_{\min} = 4u_0(u_0-1) = \frac{4(\gamma-1)}{(\gamma-2)^2}. \tag{20}$$

For $b < b_{\min}$, there are no zeros of $D$ at all; hence $D > 0$, and the general sense of the argument carries through as in Sec. 3.3. Interest then centres on situations where $b > b_{\min}$. In this case, because any zeros of $D$ must lie in $u > u_0 > 1$, the arguments previously given for the behaviour of $M^2$ versus $u$ still hold for $0 \leqslant u \leqslant u_0$, and hold unequivocally for *all* $u$ in $0 \leqslant u \leqslant \infty$ when $b < b_{\min}$.

Now consider the zeros of $N$. They can occur at

$$b = \frac{(u-1)^2[u(\gamma+1) - 2\beta]}{u[\gamma u - (\gamma+1)]}. \tag{21}$$

https://doi.org/10.1017/S0022377800008801 Published online by Cambridge University Press

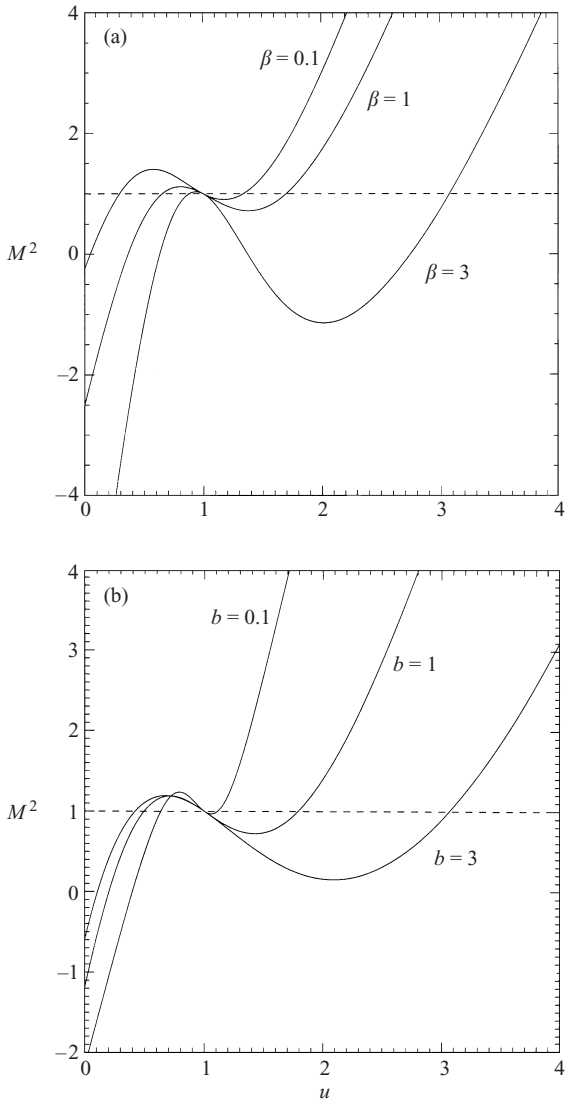



**Figure 3.** As Fig. 2, but for the intermediate case of $\gamma = 1.5$. Note in both Figs 2 and 3 that $M^2$ tends to a finite value as $u \to 0$, whereas in Fig. 1, $M^2 \to -\infty$ as $u \to 0$.

Because $b > 0$, zeros of (21) occur only under one of two conditions: either

$$u \geqslant \frac{2\beta}{\gamma + 1} \quad \text{and} \quad u \geqslant \frac{\gamma + 1}{\gamma} \tag{22a}$$

or

$$u < \frac{2\beta}{\gamma + 1} \quad \text{and} \quad u < \frac{\gamma + 1}{\gamma}. \tag{22b}$$

In general, (21) again has a minimum in situations (22a) and (22b), so that there is again a minimum value of $b$ for $N$ to have a zero. If neither (22a) nor (22b) is fulfilled then $N$ does not have a zero, and the general sense of the argument given previously can be invoked.

https://doi.org/10.1017/S0022377800008801 Published online by Cambridge University Press

More detailed descriptions of this anomalous case can then be worked through relative to particular orderings for the locations of zeros of $N$ and $D$. However, the description becomes involved, but not difficult, for arbitrary $\beta$, and for that reason is omitted here.

## 5. Compression ratios for $1 \leqslant \gamma \leqslant 2$

As well as the behaviour of the Mach number $M$, there is also the gas compression ratio $r$ to consider, which, according to (2), is given by

$$r = M^2/u. \tag{23}$$

In all cases given, there are two regimes for $u$ where $M^2 > 1$. The first regime is $u_2 \leqslant u \leqslant 1$, as sketched in Figs 1–3 for special parameter values. The second regime is always beyond $u = 1$, because the asymptotic ($u \to \infty$) value of $M^2$ is

$$M^2 \to \frac{2u^2}{b} \quad \text{for} \quad \gamma = 1, \tag{24a}$$

$$M^2 \to \frac{(\gamma+1)u}{(\gamma-1)} \quad \text{for} \quad 1 < \gamma < 2, \tag{24b}$$

$$M^2 \to 3u \quad \text{for} \quad \gamma = 2. \tag{24c}$$

In all cases $M^2$ tends to a large value. Thus, in the small-$u$ regime ($u_2 < u < 1$), where $M^2 \geqslant 1$, it follows that $r \geqslant 1$, so that one has compression of the gas. However, in the large-$u$ regime ($u > 1$), where $\infty > M^2 > 1$, initially as $M$ crosses unity and $u > 1$ one has $r < 1$, and only as $M$ increases towards its asymptotic value does $r$ eventually cross unity and lead to a high ($> 1$) compression ratio.

Thus there is a region in the high-$u$ section where $r$ represents a rarefaction ($r < 1$) before turning into a compression ($r > 1$) at higher values of $u$. Figure 4 shows the behaviour of $r$ versus $u$ for $\gamma = 1.5$ and for various values of $\beta$ and $b$. The curves are drawn only in the physical domain $M^2 > 1$. Note that the dashed line represents $r = 1$, so that the rarefaction and compression regions can be clearly seen. This rarefaction region can significantly change the cosmic-ray spectral index, as we now discuss.

## 6. Cosmic-ray spectral indices in $1 \leqslant \gamma \leqslant 2$

Combining (2) and (4), we obtain for the scattering-centre compression ratio

$$R = r\,\frac{M + H_{c,1}}{M + r^{1/2}H_{c,2}} = \frac{M}{u^{1/2}}\,\frac{M + H_{c,1}}{u^{1/2} + H_{c,2}}. \tag{25}$$

Using equations (30)–(33) of VS, the downstream cross-helicity state is

$$H_{c,2} = H_{c,1}\,\frac{(M + u^{1/2})^2|u^{1/2} - H_{c,1}|^{q+1} - (M - u^{1/2})^2|u^{1/2} + H_{c,1}|^{q+1}}{(M + u^{1/2})^2|u^{1/2} - H_{c,1}|^{q+1} + (M - u^{1/2})^2|u^{1/2} + H_{c,1}|^{q+1}}, \tag{26}$$

where $q$ denotes the spectral index of the upstream Alfvén-wave power spectrum.

https://doi.org/10.1017/S0022377800008801 Published online by Cambridge University Press

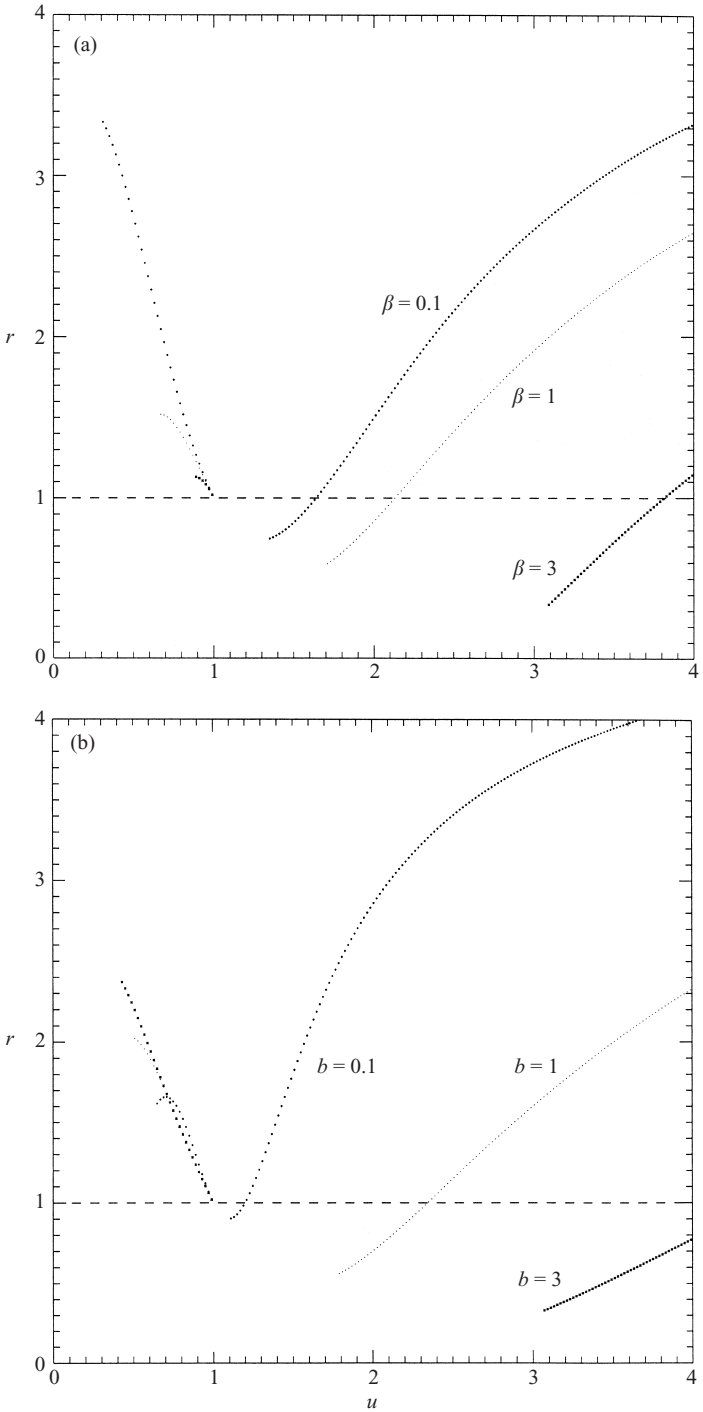



**Figure 4.** For caption, see facing page.

https://doi.org/10.1017/S0022377800008801 Published online by Cambridge University Press

Inserting (26) into (25) yields

$$R = \frac{M}{u^{1/2}}(M + H_{c,1}) \times \left[u^{1/2} + H_{c,1}\frac{(M+u^{1/2})^2|u^{1/2}-H_{c,1}|^{q+1} - (M-u^{1/2})^2|u^{1/2}+H_{c,1}|^{q+1}}{(M+u^{1/2})^2|u^{1/2}-H_{c,1}|^{q+1} + (M-u^{1/2})^2|u^{1/2}+H_{c,1}|^{q+1}}\right]^{-1} \quad (27)$$

and, from (5), the particle spectral index $\Gamma$, remembering that $M = M(u)$.

We note from (27) that only in the case of zero upstream cross helicity, $H_{c,1} = 0$, is the scattering-centre compression ratio $R$ the same as the gas compression ratio $r$. In Figs 5 and 6 for the upstream cross-helicity states $H_{c,1} = -1$ and $+1$, we calculate the variations of the scattering-centre compression ratio $R$ and the cosmic-ray spectral index $\Gamma$ versus the parametric variable $u$ for values of $\gamma = 1.5$, for a wave spectral index $q = \frac{5}{3}$, and for various values of $b$ and $\beta$.

## 7. Summary and conclusions

In this work, we have investigated the properties of turbulent adiabatic shock waves and the consequences for diffusive acceleration of cosmic-ray particles. Perhaps the most important points to be gleaned from these investigations are the

**Figure 4.** Plots of the gas compression ratio $r$ versus $u$ for $\gamma = 1.5$: (a) for $b = 0.6$ for various values of the plasma beta $\beta$; (b) for $\beta = 0.6$ for various values of the turbulence parameter $b$. The curves are drawn only for the physically acceptable regimes where $M^2 \geqslant 1$. The dashed line is $r = 1$, showing that both compression and rarefaction regions exist when the wave energy is included in the shock balance equation (3). Note that in the case of zero upstream cross helicity, the particle spectral index $\Gamma$ is just $(r + 2)/(r - 1)$, so that in the regions of rarefaction, $\Gamma < 0$, implying an increasing energy distribution of particles – the 'pile-up' problem detailed by Schlickeiser (1984).

**Figure 5** (pages 470 and 471). Plots of the scattering-centre compression ratio $R$ at $\gamma = 1.5$ and a wave spectral index of $q = \frac{5}{3}$, versus $u$ for various values of the plasma beta $\beta$ and the turbulence parameter $b$, and different upstream wave cross helicities $H_{c,1}$. Curves are shown in the physical domain $M^2 \geqslant 1$: (a) $H_{c,1} = +1$ and $b = 0.6$ for $\beta = 0.1, 1, 3$; (b) $H_{c,1} = +1$ and $\beta = 0.6$ for $b = 0.1, 1, 3$; (c) $H_{c,1} = -1$ and $b = 0.6$ for $\beta = 0.1, 1, 3$; (d) $H_{c,1} = -1$ and $\beta = 0.6$ for $b = 0.1, 1, 3$. Note that in (a), for $\beta = 0.1$ and $u < 1$, a formally negative value of $R$ occurs – in which case, the solid line represents $|R|$. In (b), this happens for all values of $b$, indicated by the solid, dotted, and dashed lines, respectively.

**Figure 6** (pages 472 and 473). Plots of $1/\Gamma$, the inverse of the particle spectral index, versus $u$ at $\gamma = 1.5$ and a wave spectral index of $q = \frac{5}{3}$, for various values of the plasma beta $\beta$ and the turbulence parameter $b$, and different upstream wave cross helicities $H_{c,1}$. Curves are shown in the physical domain $M^2 \geqslant 1$: (a) $H_{c,1} = +1$ and $b = 0.6$ for $\beta = 0.1, 1, 3$; (b) $H_{c,1} = +1$ and $\beta = 0.6$ for $b = 0.1, 1, 3$; (c) $H_{c,1} = -1$ and $b = 0.6$ for $\beta = 0.1, 1, 3$; (d) $H_{c,1} = -1$ and $\beta = 0.6$ for $b = 0.1, 1, 3$. Note the regions where $\Gamma$ is negative, representing a particle spectrum increasing with increasing energy. At high values of $u$ (strong shocks), all curves tend to $\Gamma = \frac{1}{2}(3\gamma - 1)$, which is $\frac{7}{4}$ here ($1/\Gamma \simeq 0.57$).

https://doi.org/10.1017/S0022377800008801 Published online by Cambridge University Press

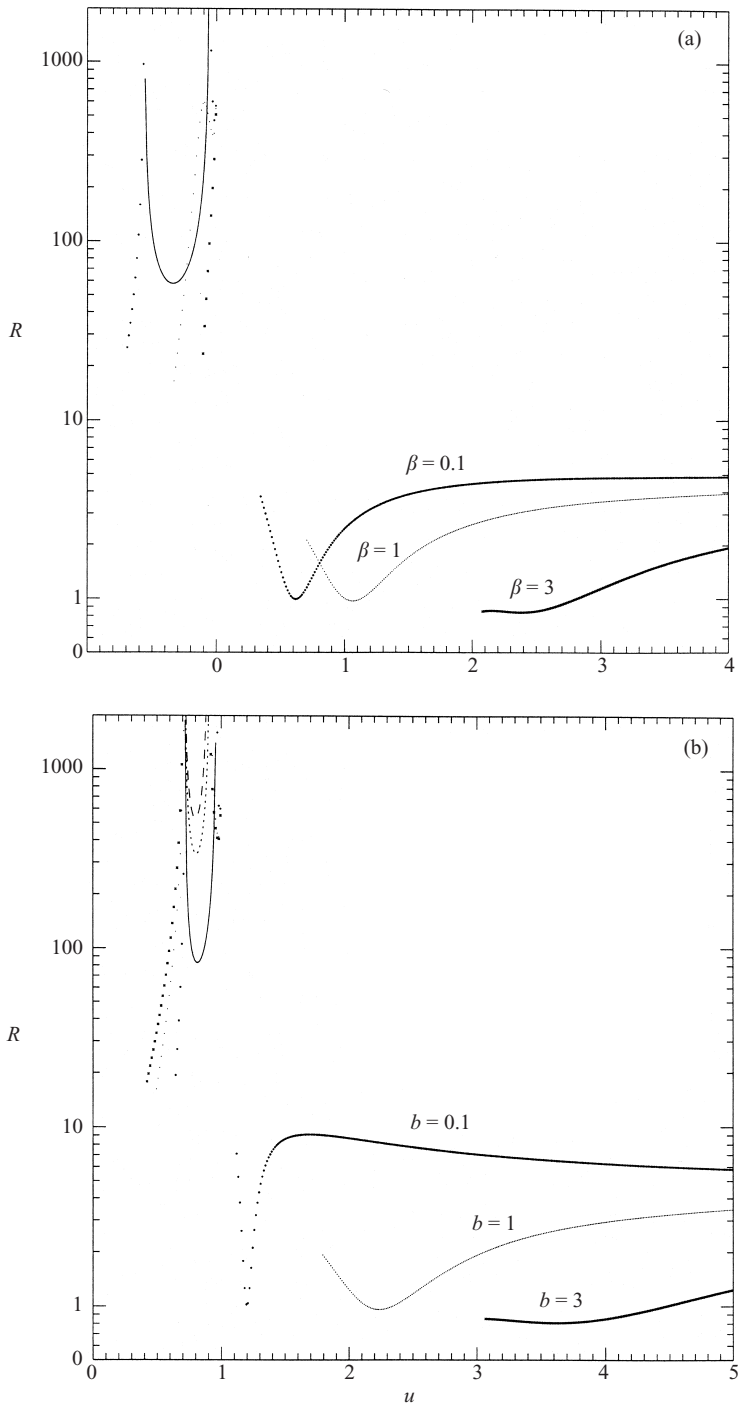



**Figure 5 (a, b).** For caption, see page 469.

https://doi.org/10.1017/S0022377800008801 Published online by Cambridge University Press

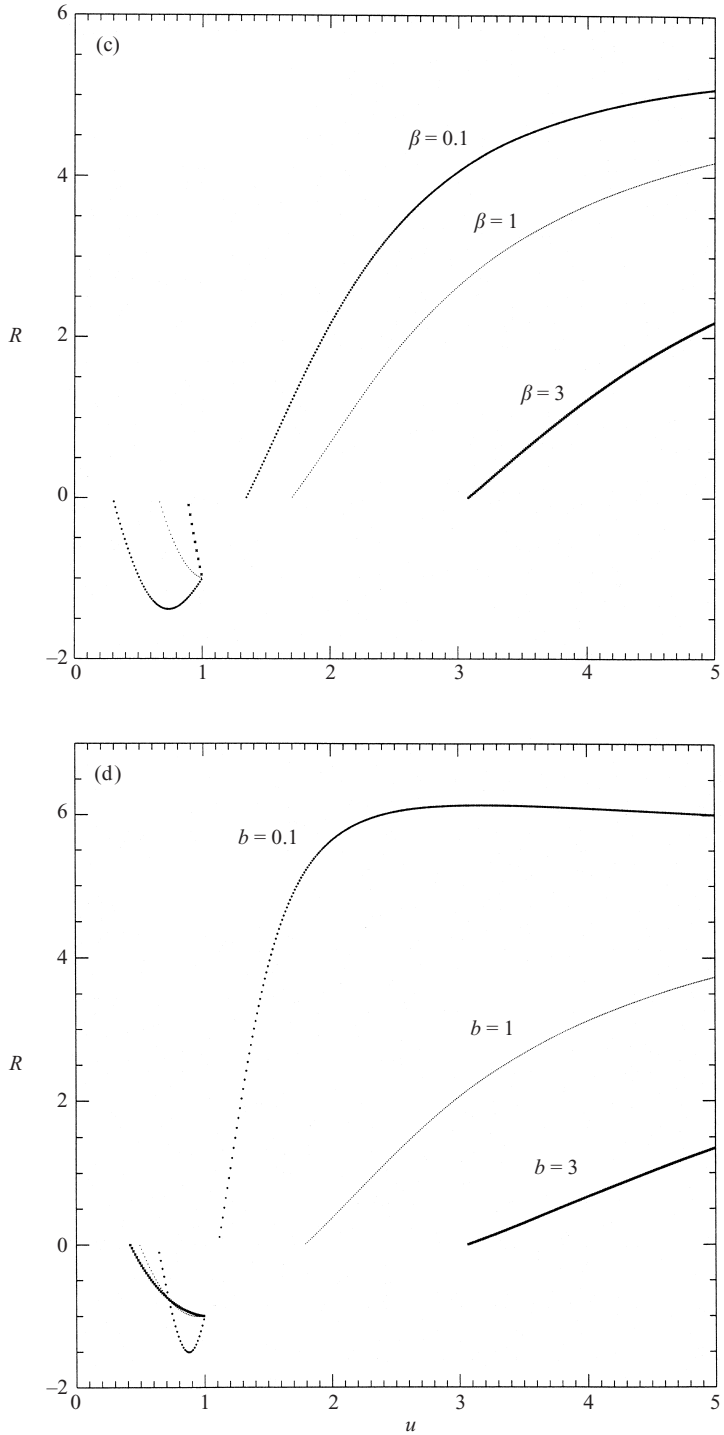



**Figure 5 (c, d).** For caption, see page 469.

https://doi.org/10.1017/S0022377800008801 Published online by Cambridge University Press

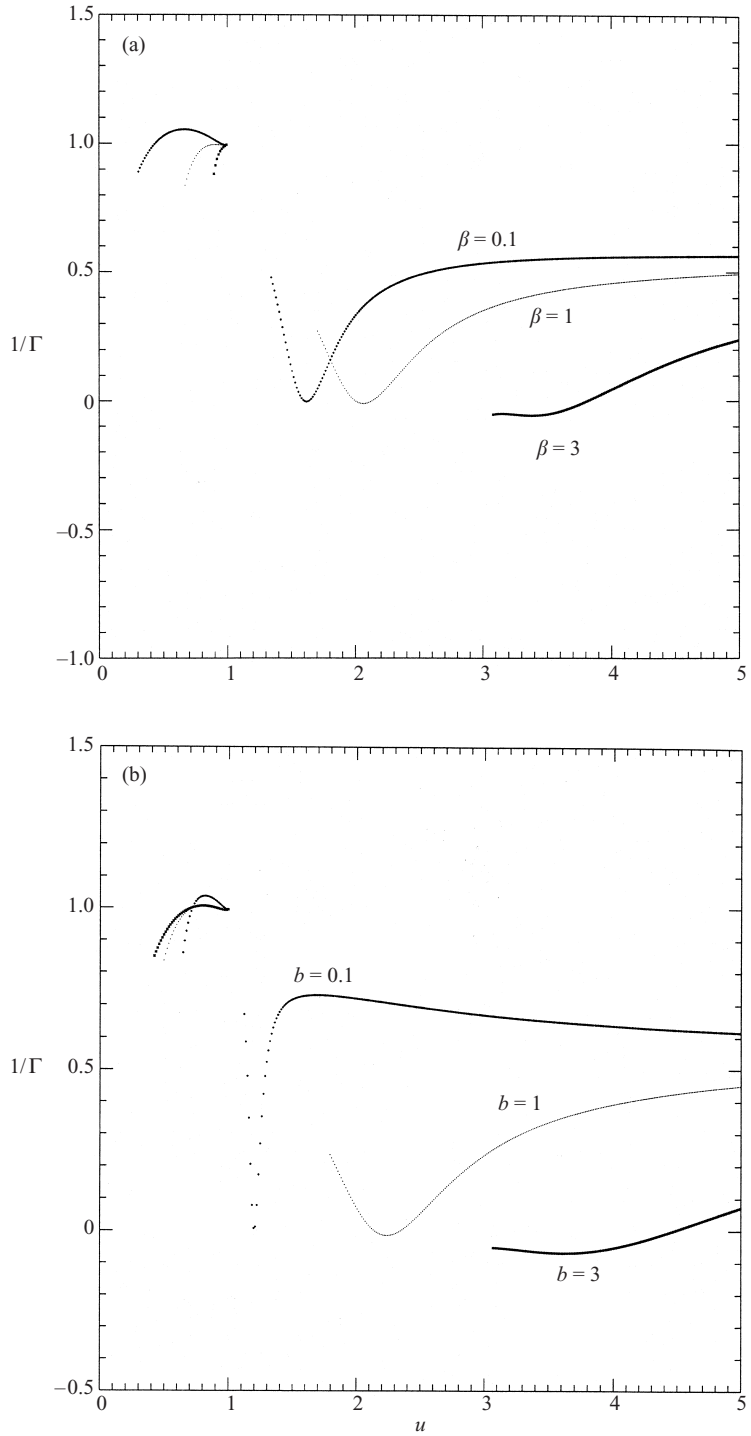



**Figure 6 (a, b).** For caption, see page 469.

https://doi.org/10.1017/S0022377800008801 Published online by Cambridge University Press

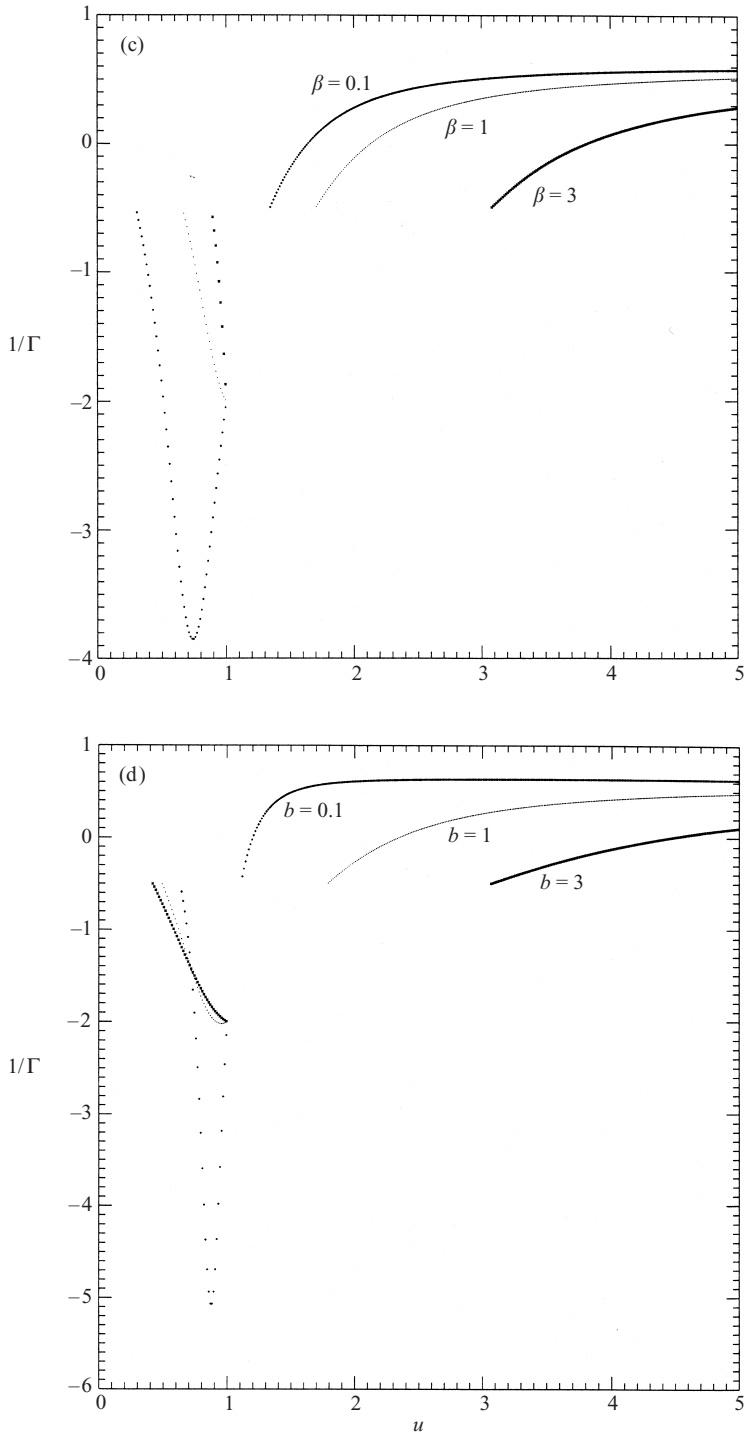



**Figure 6 (c, d).** For caption, see page 469.

https://doi.org/10.1017/S0022377800008801 Published online by Cambridge University Press

following:

(i) the absence of a switch-on shock;

(ii) the domain in $0 < u < 1$ of the parametric variable $u$ where $M^2 > 1$;

(iii) the domain in $u > 1$ where a gas compression ratio less than unity exists (i.e. a rarefaction domain);

(iv) the difference between the scattering-centre compression ratio and the gas compression ratio for all upstream wave-helicity values except for the isolated case $H_{c,1} = 0$;

(v) the presence of anomalous domains where the cosmic-ray particle spectral index can be negative.

All of these results are brought about by including the upstream and downstream turbulent wave energies in the shock balance structure. Without the waves, none of the effects persists. It is, arguably, this general point that the present calculations speak to most strongly. It would seem that the rich diversity of new phenomena at and in the neighbourhood of collisionless shocks, brought about by inclusion of waves, deserves a more thorough and detailed investigation.

*Acknowledgements*

We acknowledge partial support by the Deutsche Forschungsgemeinschaft through Sonderforschungsbereich 191 and by the Bundesministerium für Bildung und Forschung through Deutsches Zentrum für Luft- und Raumfahrt, Grant 50 OR 0006.

## References

Achterberg, A. and Blandford, R. D. 1986 *Mon. Not. R. Astron. Soc.* **218**, 551.
Blandford, R. D. and Eichler, D. 1987 *Phys. Rep.* **154**, 1.
Boyd, T. J. M. and Sanderson, J. J. 1969 *Plasma Dynamics*. Thomas Nelson, London.
Dröge, W., Lerche, I. and Schlickeiser, R. 1987 *Astron. Astrophys.* **178**, 252.
Drury, L. O. C. 1983 *Rep. Progr. Phys.* **46**, 973.
Jones, F. C. and Ellison, D. C. 1991 *Space Sci. Rev.* **58**, 259.
Kennel, C. F., Coroniti, F. V., Scarf, F. L. et al. 1986 *J. Geophys. Res.* **91**, 11917.
McKenzie, J. F. and Westphal, K. O. 1969 *Planet. Space Science* **17**, 1029.
Schlickeiser, R. 1984 *Astron. Astrophys.* **136**, 227.
Schlickeiser, R. and Fürst, E. 1989 *Astron. Astrophys.* **219**, 192.
Schlickeiser, R., Campeanu, A. and Lerche, I. 1993 *Astron. Astrophys.* **276**, 614.
Scholer, M. and Belcher, J. W. 1971 *Solar Phys.* **16**, 472.
Vainio, R. and Schlickeiser, R. 1998 *Astron. Astrophys.* **331**, 793.
Vainio, R. and Schlickeiser, R. 1999 *Astron. Astrophys.* **343**, 303.

https://doi.org/10.1017/S0022377800008801 Published online by Cambridge University Press